June 2023

Constraining the Higgs width in Higgs production associated with a top quark pair

Benjamin Dahlén

Department of Physics, Lund University

Bachelor thesis supervised by Rikkert Frederix

LUND
UNIVERSITY

Abstract

In this thesis we study the width of the Higgs boson in the process $pp \to t\bar{t}4l$ at LO using MadGraph5_aMC@NLO to generate the events. The contributions including the Higgs signal, continuum background and interference were considered in order to calculate the expected number of events in a broad range of four-lepton invariant masses. Due to strongly enhanced off-shell contributions an upper bound on the Higgs width could be derived. By assuming that the coupling constants scale by a multiplicative constant, allowing the on-shell cross section to be compatible with the Standard Model for different Higgs widths, we calculate the expected number of events in the off-peak region using an integrated luminosity of 3000 fb^{-1}. Considering the statistical uncertainty of the expected number of events for the process with the SM width we find an upper bound on the Higgs width $\Gamma_H \leq 3.54\,\Gamma_H^{SM}$ at the 95% confidence level. This result translates into an upper limit on the branching ratio to invisible final states $BR_{inv} \leq 0.47$. We believe that the result can be improved by a more careful selection of the four-lepton invariant mass range. The major assumptions we use are that the top quarks can be perfectly reconstructed from their decay products and that we have an ideal detector. The cross section for this process is very small and therefore it is not particularly competitive to the limit on the Higgs width that can be derived from $pp \to H \to 4l$ not including the top quarks. However, it still provides additional information which improves the understanding of the Higgs width.

Popular Science Summary

The Standard Model of particle physics is the most promising candidate we have for a theory of everything; a theory that would be able to predict everything in our universe. There are four fundamental forces in nature: the electromagnetic force responsible for electric and magnetic fields and chemical processes, the weak force responsible for the beta decay, the strong force which holds the nucleus together inside atoms and the gravitational force. The Standard Model describes the first three fundamental forces mentioned and how the smallest constituents of matter interact via these forces. Gravity is not included for the simple reason that we do not yet know how to incorporate gravity into the mathematical framework of the Standard Model.

There are two types of particles in our universe: matter particles that make up you, me and everything around us, such as electrons, protons and neutrons, and then there are the force carrier particles which mediate the fundamental forces, such as the photon responsible for the electromagnetic force. All of these particles except the photon and the gluon (carrier of the strong force) have mass. What puzzled scientists in the early 60s was the fact that the carriers of the weak force (the Z and W bosons) were experimentally observed to have mass which was not consistent with the current theory. This was a mystery until 1964, when Peter Higgs, François Englert and Robert Brout provided a theory that explained how particles acquire mass through the so-called Higgs mechanism. This mechanism explains how particles interact with the Higgs field and by doing so, gain mass. The mediator of the Higgs field is the Higgs boson. Finding that particle was crucial in order to justify the Higgs mechanism. Finally, in 2012, 50 years later, the Higgs boson was discovered at CERN in Geneva. This was a remarkable discovery that earned Peter Higgs and François Englert the Nobel Prize in 2013.

As most particles in the Standard Model, the Higgs boson is an unstable particle; it will exist only a fleeting moment before disintegrating into other lighter particle species. There is a direct connection between a particles lifetime and its uncertainty in mass; a property called the decay width of the particle. The width tells us how probable it is for a particle to decay to other lighter particles or equivalently, how short its lifetime is. My thesis aims to investigate the width of the Higgs boson in a specific process which has not been studied before, in order to set a boundary on how large the Higgs width can be. This will be done by simulating a proton-proton collision where the Higgs boson is produced together with a top quark pair, which is the heaviest particle in the Standard Model. This will be done with a computer program that is able to perform simulations of collisions similar to those produced at CERN. Such analyses have been done with real data from particle accelerators at CERN for other processes to gain more insight into the properties of the Higgs boson. The goal is to establish that the measured Higgs boson is the same as the one predicted from the Standard Model. If the decay width proves to be larger than the prediction it would indicate that there is physics beyond the Standard Model. This would potentially lead to new physics with the opportunity to unravel some of the mysteries of our universe.

Contents

1 Introduction

In 1964 a phenomenon called the Brout-Englert-Higgs mechanism was postulated. It provided a description that explained how the fundamental particles in the Standard Model (SM) [1] acquire mass by coupling to the Higgs field [2, 3, 4]. Almost a half century later, in 2012, a Higgs-like particle with mass $m_H \approx 125$ GeV was discovered at the Large Hadron Collider (LHC) at CERN by the ATLAS and CMS collaborations [5, 6]. The discovery mode was from proton-proton (pp) collision where the Higgs-like particle was produced from gluon fusion through a top quark loop and then decayed to two photons. This decay mode occurred in one out of 2000 events [7]. The discovery earned Peter Higgs and François Englert the Nobel Prize in 2013. The Higgs mechanism was a remarkable achievement. Most importantly it solved the problem that the gauge bosons of the weak interaction (Z and $W^{\pm}$) were observed to be massive and provided an explanation of how they acquired mass as a result of spontaneous symmetry braking. Furthermore, the mass of the fermions could also be explained and are included in the theory with a slight variation of the same mechanism which also was a great achievement.

Since the discovery in 2012 a lot has been learned about the properties of the Higgs boson. Apart from its mass, we know that it is a scalar boson with even parity [8]. To study and gain deeper understanding of the properties of the Higgs boson is a major goal in particle physics and consequently a highly active research area. With the future developments and upgrades to the LHC and in particular the High Luminosity LHC project, scientists hope to acquire more Higgs events to reduce the uncertainties in the measurements and enhance the understanding of the various properties of the Higgs boson. One such property is the width, Γ. As the majority of the fundamental particles in the Standard Model, the Higgs boson is an unstable particle; it has a short lifetime, existing only for a fleeting moment. The width is proportional to the inverse of the lifetime and the SM prediction of the decay width of the Higgs boson is $\Gamma_H^{SM} = 4.1$ MeV [9]. That is a tiny width; three orders of magnitude smaller than the widths of the Z and $W^{\pm}$ bosons for comparison. The smallness of the width of the Higgs boson provides difficulties in actually measuring its value. In the case of the Z and W bosons which have relatively broad resonances, the width can be obtained directly by measuring the shape of the Breit-Wigner peak. The Breit-Wigner peak of the Higgs boson is too narrow to resolve experimentally, which makes it impossible, at least with the current techniques, to directly measure its width.

Fortunately, the width changes distributions and cross sections indirectly and in particular the ratio of the so-called on-shell and off-shell regions of the production cross section are sensitive to the width. By considering the off-shell contribution to the cross section where the Higgs boson mass is far from its nominal value and relating it to the on-shell cross section, the Higgs width can be obtained. This lies at the core of this thesis and will be covered and explained in greater detail in the theory section 2. Measuring the off-shell production and relating it to the on-shell production is a technique that has previously been utilized to determine Γ_H. For instance, in October 2022, the CMS collaboration measured

the total width of the Higgs boson to be $\Gamma_H = 3.2^{+2.4}_{-1.7}$ MeV where they considered the decay to two Z bosons [10]. So far it seems that the Higgs production cross section in different productions and decay channels observed at the LHC is consistent with the SM. It is conventional to translate this result into a statement about the coupling constants to the Higgs boson. However, such a translation is only possible if we assume that Γ_H is equal to the SM value of the width. A goal in particle physics is therefore to reduce the uncertainties of the width, in particular to decrease the upper bound on the width as much as possible. Future developments of particle accelerators will allow for larger collision energies and a larger integrated luminosity such that more events can be generated and more precise measurements can be conducted. New production modes can also be considered which might yield better results and lower uncertainties on Γ_H. A deviation from the predicted SM width would indicate new physics beyond the Standard Model (BSM).

This thesis aims to derive an upper bound on the Higgs width by considering a specific production mode that has not previously been studied. The production channel of interest is that of Higgs production together with a top quark pair from pp collision where Higgs then decays to two Z bosons which decay to 4 leptons ($4l$). This process will be generated using the computer program MadGraph5_aMC@NLO [11] which aims at providing all elements necessary for SM and BSM phenomenology. Three different signals will be considered. The *total signal* which is the one that would be measured in a detector: $pp \to t\bar{t}4l$. The total signal is made up of the following three contributions: *H signal* which only includes events with Higgs as an intermediate particle, *continuum background signal* where Higgs is excluded, and *interference* which is the interference between the amplitudes of the first two signals. These three terms will be generated separately and the invariant mass for the final state leptons will be calculated and presented in histograms for the processes. Thereafter, an upper bound on the Higgs width will be derived by first considering solely the H signal and subsequently considering the total signal. The central idea of this thesis is that the on-shell cross section for different widths can be normalized such that they are always compatible with the SM cross section. That is justified because on-shell cross section measurements at the LHC can be compatible with the SM although the width and coupling constants are not.

This thesis is structured as follows. In section 2 an overview of the relevant physics are introduced and theoretical concepts are explained. In subsection 2.1, 2.2 and 2.3, the width and the cross section for Higgs production including the on-shell and off-shell contributions are explained, and the theory of constraining the branching ratio is introduced. A brief overview of the theoretical bases and methodology of computation in MadGraph5_aMC@NLO is given in subsection 2.4. To end the theory section, a description of how an upper bound on Γ_H can be obtained using statistical uncertainty is presented in subsection 2.5. The numerical method of generating the desired processes and calculating the invariant mass of the final state leptons from the event files are described in section 3. In section 4 the results including the histograms and the upper limit on Γ_H are presented and the approximations made and the implications of the results are discussed. Lastly, in section 5, a conclusion and a future outlook is given.

2 Theory

2.1 Breit-Wigner Resonance and Decay Widths

The Heisenberg's uncertainty principle provides a connection between the lifetime and the uncertainty in mass for an unstable particle; this property is known as the width Γ of the particle. The width is directly related to the lifetime τ as $\Gamma = 1/\tau$ (in natural units). By measuring the energy E_i and momentum $\mathbf{p}_i$ of the decay products of a resonant particle, the invariant mass can be calculated:

$$M = \sqrt{(\sum_i E_i)^2 - |\sum_i \mathbf{p}_i|^2}, \tag{2.1}$$

where the sum ranges over all decay products. The invariant mass translates to the mass of the resonant particle. The observed mass will not be constant across a series of measurements, instead the possible values of its mass are distributed according to a relativistic Breit-Wigner distribution. This is called a Breit-Wigner resonance [12]. The nominal mass value corresponds to the maximum value of the bell curve, and the full width at half maximum of the peak is the decay width of the unstable particle (see Figure 1).

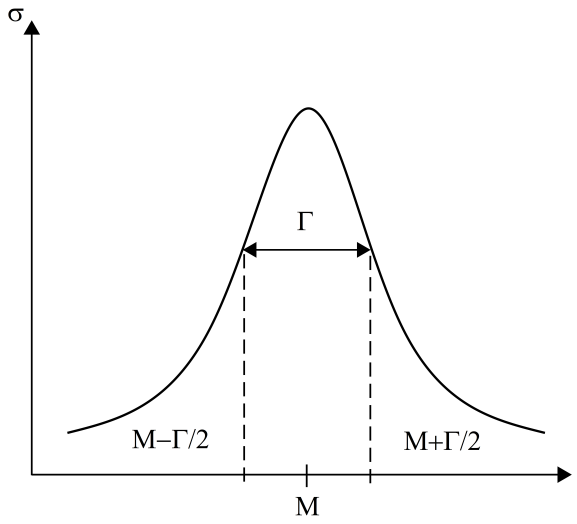

Figure 1: Graphical representation of a Breit-Wigner resonance. M is the nominal mass value and Γ is the decay width given by the full width at half maximum of the bell curve.

Particles are said to be *on-shell* if their mass is close to the nominal mass value; the resonant region. If the mass value of the resonant particle takes a value far from the peak region it is said to be *off-shell*. Due to the shape of the Breit-Wigner distribution it is far more probable for particles to be produced on-shell if energy and momentum conservation

allow it. Furthermore, the total decay width is affected by the number of possible decay products; more decay channels results in a larger total width. The ratio between the width for a specific decay channel and the total width is called the branching ratio:

$$BR(R \to AB) = \frac{\Gamma_R^{AB}}{\Gamma_R^{TOT}}, \tag{2.2}$$

where Γ_R^{AB} is the partial width of particle R decaying to particles A and B and Γ_R^{TOT} is the sum of all partial widths; the total decay width. The branching ratios determine the decay signatures that allow the resonant particle to be detected. If there are additional BSM decay products that the Higgs boson can decay to it would result in a larger total width Γ_H than predicted from SM and consequently the branching ratios to e.g. photon-photon or ZZ would be smaller.

2.2 Cross Sections, on-shell and off-shell contributions

The cross-section of a process is a measure of the probability that a certain process occurs. The cross section for a specific process is determined by the absolute square of the matrix element M. Considering the Feynman diagrams describing the process in interest, the Lagrangian field theory provides the rules to write the matrix element by combining propagators and vertices.

The properties of particles can be experimentally probed by colliding hadrons, usually protons, at high energies at particle accelerators. Hadrons are composite particles and thus the production cross section becomes more difficult to calculate than if fundamental particles were to collide. Nonetheless, there are so-called master formulae describing hadronic cross sections. Given a partonic subprocess cross section $\hat{\sigma}$, the production cross section for a general process at a proton-proton collider $\sigma(pp \to X)$ can be expressed by the following master formula [13]:

$$\sigma_{pp\to X} = \sum_{i,j} \int dx_1 dx_2 f_i(x_1, Q^2) f_j(x_2, Q^2) \hat{\sigma}_{ij}(\hat{s}, Q^2), \tag{2.3}$$

where the sum runs over all the parton types inside the hadron that can interact for the given process. The function $f(x, Q^2)$ is the parton distribution function (PDF) and represents the probability to find a parton of type i carrying a momentum fraction x inside a proton probed at the energy scale Q^2. The partonic cross section $\hat{\sigma}_{ij}(\hat{s}, Q^2)$ is given by $\overline{|M|^2}$ times the phase space terms divided by a flux factor, and it is a function of $\hat{s} = x_1 x_2 s$ where s is the center of momentum energy squared.

A possible Higgs production mode from pp collisions is from gluon fusion via a top quark loop where the Higgs boson decays to two Z bosons and then to 4 leptons described by the Feynman diagram in Figure 2.

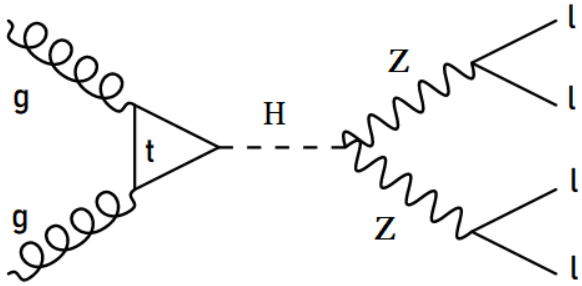

Figure 2: A possible Feynman diagram for $pp \to H \to ZZ \to 4l$ where l denotes an electron or muon. This kind of process we refer to as the H signal.

The matrix element for this particular process is found to be proportional to

$$M \propto \frac{g_i g_f}{M_{4l}^2 - m_H^2 + i\Gamma_H m_H}, \tag{2.4}$$

where g_i and g_f are the Higgs boson coupling constants to the initial and final states respectively and $\frac{1}{M_{4l}^2 - m_H^2 + i\Gamma_H m_H}$ is the propagator term for the resonant Higgs boson where M_{4l} is the invariant mass of the final state leptons and m_H is the Higgs boson mass. The differential cross section as a function of M_{4l} can be expressed as [14]

$$\frac{d\sigma_{pp\to H\to 4l}}{dM_{4l}^2} \propto \frac{g_i^2 g_f^2}{(M_{4l}^2 - m_H^2)^2 + m_H^2\Gamma_H^2}. \tag{2.5}$$

This process receives the dominant contribution from the resonant region where the Higgs boson is on-shell; $|M_{4l}^2 - m_H^2| \lesssim m_H\Gamma_H$. In the narrow width approximation [15, 16, 17] the integral of Eq. 2.5 gives the on-shell production cross section for $pp \to H \to 4l$ and it is proportional to

$$\sigma^{on-shell} \propto \frac{g_i^2 g_f^2}{\Gamma_H}. \tag{2.6}$$

The on-shell cross section is proportional to the inverse of the Higgs width, but this is still not enough to unambiguously extract the width from a cross section measurement due to the Breit-Wigner peak being too narrow to experimentally resolve. However, the total production cross section for the process also receives off-shell contributions. Note that the mass of two Z bosons (≈ 180 GeV) is larger than the nominal mass of the Higgs boson. If the Higgs boson is on-shell, one or both of the Z bosons have to be off-shell and if the Higgs boson is off-shell the Z bosons are allowed to be on-shell. The production rate of off-shell Higgs bosons above the Z boson pair production threshold is enhanced compared to what one would expect from the shape of Breit–Wigner resonance of the Higgs boson alone. The off-shell production cross section is proportional to

$$\sigma^{off-shell} \propto g_i^2 g_f^2. \tag{2.7}$$

Note that an on-shell Z boson contributes significantly less to the total cross section than if Higgs is on shell, due to Γ_Z being almost 3 orders of magnitude larger than Γ_H ($\Gamma_Z = 2.495 \pm 0.002$ GeV [18]). Nevertheless, there are contributions to the total cross section in $pp \to H \to ZZ$ from off-shell Higgs bosons given by Eq. 2.7 and they are enhanced since the Breit-Wigner distribution of either Higgs or Z maximizes at its respective nominal mass, creating a Breit-Wigner shape of the form presented in Figure 4.

The off-shell cross section $\sigma^{off-shell}$ is not dependent on the Higgs width. However, the on-shell and off-shell cross sections can be related to derive an upper bound on the Higgs width. If we assume that the coupling constants and Γ_H scale by a common multiplicative constant λ in a BSM theory, $\sigma^{on-shell}$ remains the same when scaled by λ such that it coincides with the expected SM value in all channels. It can be concluded that LHC data allows for infinitely many solutions of Γ_H, the Higgs boson couplings, and the branching ratios to different decay products when considering the resonant region. In the next subsection 2.3 it is explained how this can be used to set constraints on the branching ratio. On the contrary the off-shell production cross section would increase linearly with λ when scaling the cross section such that the on-shell cross section remains the same for all Γ_H. Therefore, $\sigma^{off-shell}$ can be bounded from above by the total number of events observed in $pp \to ZZ \to t\bar{t}4l$ which is the process considered in this thesis. How this is done is explained in subsection 2.5.

The events from $pp \to ZZ \to 4l$ do not necessarily include a Higgs boson. An amplitude given by the Feynman diagram in Figure3 is possible and referred to as the continuum background. These two amplitudes corresponding to the Feynman diagrams in Figure 2 and Figure 3 can interfere with each other. The interference is numerically irrelevant in the peak but it contributes significantly to the off-peak region and changes the expected number of events in that region [17].

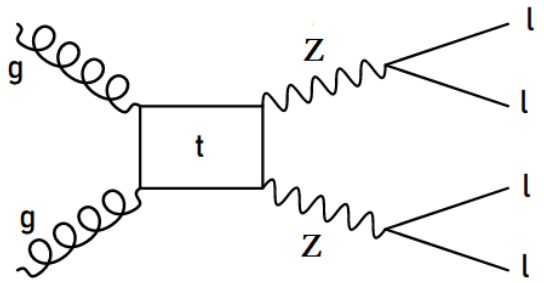

Figure 3: Feynman diagram of the Continuum background signal.

The total signal from $pp \to ZZ \to 4l$ which is the signal that can be measured at LHC consists of the H signal (Figure 2), the continuum background (Figure 3) and the interference. The cross section from each of these three contributions adds up to the total cross

section as

$$\sigma_{tot} = \sigma_H + \sigma_C + \sigma_{int}. \tag{2.8}$$

The cross section of the continuum background (σ_C) and interference (σ_{int}) scale differently from the H signal. In terms of the Higgs boson coupling constants g_i and g_f, the cross sections of these contributions is proportional to

$$\sigma_C \propto 1 \qquad \sigma_{int} \propto g_i g_f. \tag{2.9}$$

Note that the interference scales as the square root of the H signal in the off-shell region given by Eq. 2.7. The continuum background contributes to an enhanced off-peak cross section, compared to the off-shell cross section of the H signal alone, which corresponds to a Breit-Wigner shape of the total signal represented by Figure 4.

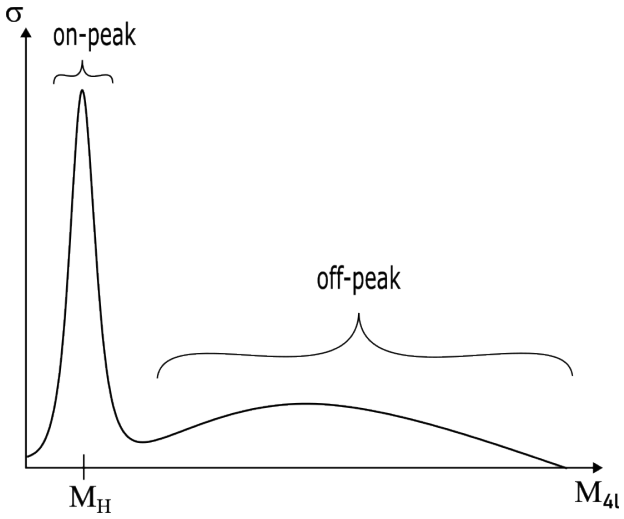

Figure 4: Schematic figure of the shape of the Breit-Wigner distribution of $pp \to ZZ \to 4l$. The cross section is a function of the invariant mass of $4l$. the large narrow peak corresponds to the resonant region ($M_H \approx 125$ MeV) and the lower flattened out curve represents the off-peak region where Higgs is off-shell and contributions from the continuum background and interference.

So far, the process where the Higgs boson is produced from pp collision and the decay $H \to ZZ \to 4l$ have been considered when deriving the cross sections. The production of the top quarks together with the Higgs boson which is studied in this thesis has so far not been considered. The additional top quarks do not change the expressions derived because the Higgs boson still decays to the same final states. However, the top quarks will alter the measured cross section because much energy goes into the production of the heavy top quarks as they are the most massive particles in the SM with a mass $m_t = (172.22 \pm 0.73)$ GeV [19]. Also, tree level diagrams are possible in the process $pp \to ZZ \to t\bar{t}4l$. The only possible decay for the Higgs boson in this process is to two Z bosons. However, for the continuum background where Higgs is excluded, virtual photons can appear in the Feynman diagrams instead of Z bosons.

2.3 Constraining the branching ratio in a BSM theory

In a BSM theory the Higgs width can be expressed as

$$\Gamma_H = \Gamma_{inv} + \sum_{i \in vis} \Gamma_i \tag{2.10}$$

where Γ_{inv} corresponds to the width from decay modes not included in SM that are assumed to be invisible. Likewise, the Standard Model Higgs width can be written as the sum of the partial widths from all possible decay products in the SM:

$$\Gamma_H^{SM} = \sum_{i \in vis} \Gamma_i^{SM}. \tag{2.11}$$

If an on-shell Higgs boson cross section consistent with the SM was to be measured the following should be true:

$$\frac{g_i^2 g_f^2}{\Gamma_H} = \frac{g_{i,SM}^2 g_{f,SM}^2}{\Gamma_H^{SM}}, \tag{2.12}$$

to keep all narrow-width Higgs boson production cross-sections to be the same as in the SM. This implies that even if $\sigma = \sigma_{SM}$ it is not necessarily true that the couplings g_i, g_f and the Higgs width Γ_H are equal to their SM values. Hence, a measured on-shell cross section can be compatible with the SM even if the values of Γ_H and the couplings are not. In addition, keep in mind that for most Higgs processes the Higgs boson is exclusively on-shell (e.g. $H \to \gamma\gamma$). Now assume that all Higgs couplings scale by identical factors μ relative to their SM values; $g = \mu g_{SM}$. Also note that $\Gamma_{i \in vis} \propto g_i^2$. From these conditions and Eq. 2.10, 2.11 and Eq. 2.12 it can be found that the Higgs width and the branching ratio to invisible final states satisfy the following constraint [14]:

$$\Gamma_H (1 - BR_{inv})^2 = \Gamma_H^{SM}. \tag{2.13}$$

This constraint translates into an expression for the upper boundary on the branching ratio to invisible final states BR_{inv} given by

$$BR_{inv} = 1 - \sqrt{\frac{\Gamma_H^{SM}}{\Gamma_H}}. \tag{2.14}$$

If there are decay channels beyond the Standard Model the Higgs width Γ_H would be larger than Γ_H^{SM} and it would allow for an upper bound on the branching ratio to these BSM decay product given by Eq. 2.14. An upper bound on the Higgs width can be derived by using the total number of events observed in the desired process in a broad range of the invariant mass of the final state particles which will be discussed in subsection 2.5.

2.4 MadGraph5_aMC@NLO

The computer program MadGraph5_aMC@NLO is a Monte Carlo event generator able to perform computations of tree-level amplitudes and one-loop amplitudes for arbitrary processes. MadGraph5_aMC@NLO is a part of the madgraph family and it is the new version of both MadGraph 5 and aMC@NLO that unifies leading order (LO) or tree level, and next-to-leading order (NLO) developments in the previous programs. The central idea of the program is that the cross section computations are essentially independent of the process, regardless of the theory that is considered and the perturbative order. On the other hand, matrix elements are evidently process dependent, but they can be computed starting from Feynman rules, i.e. a very limited number of formal instructions. Therefore, the program is constructed as a so-called meta-code; a code writing a code that computes the desired process. In this case it is a Python codes that writes a Python, C++ or Fortran code. Two ingredients are needed for this to work: a theory model, and a set of process independent building blocks. The theory model corresponds to the Lagrangian of the theory and its free parameters such as particle masses and coupling constants. Given a Lagrangian, its Feynman rules are derived which MadGraph5_aMC@NLO will use to construct the matrix elements. At the leading order this process is fully automated in a package called FeynRules [20]. To compute NLO cross sections there are additional difficulties involved which will not be discussed in this thesis. The process specific code is built by first writing the matrix elements and then minimal editing of the process independent building blocks. The latter corresponds to assigning appropriate values to particle identities such that definite values of the number of particles and masses can be selected. Note that the user will not play any role in any of these operations as they are all performed automatically.

To access MadGraph5_aMC@NLO [11] one executes the following command in a terminal shell:

```
./bin/mg5_aMC
```

To compute a cross section three commands are executed in the prompt:

```
MG5_aMC> generate process
MG5_aMC> output
MG5_aMC> launch
```

There are four options available following the command `generate` but the only mandatory one which will be considered in this thesis is *process* which refers to the actual process one needs to generate. This is done by simply listing the initial and final state particles separated by the `>` sign. For example if one were to generate a *pp* collision to a top and an anti-top quark, the following syntax is used:

```
MG5_aMC> generate p p > t t~
```

There are five process-generation syntax refinements that allows for certain requirements and restrictions to the process. Two of them relevant to this project are presented in Table 1 where the first one demands that at least one particle of type `x` will be in an s-channel (time-like channel) and the second syntax discards all particles of type `x` featured anywhere.

syntax	example
`> x >`	`p p > Z > e+ e-`
`/ x`	`p p > e+ e- / Z`

Table 1: This table presents syntax refinements for process generation and examples of processes with a Z boson.

When the desired process has been generated it can be saved in a directory with the `output` command and then by executing the `launch` command the so-called *running mode* environment is accessed. In the running mode environment the run specific options can be set by editing two cards: the *param* card which can be entered by typing `1` in the prompt and the *run* card, entered by typing `2`. In the param card properties of the particles present in the processes are specified and can be edited, such as mass and decay width. The default parameters are the SM values. The run card contains information about the collision and detection such as limits of the transverse momentum of charged leptons, pseudo-rapidity, parameters related to decay widths, etc. The transverse momentum p_T is the momentum perpendicular to the collision axis and the pseudo-rapidity is given by

$$\eta = -ln\left(\tan\theta/2\right) \tag{2.15}$$

where θ is the angle between the particles' momentum vector and the collision axis. The number of events to be generated and the beam energy can also be edited in this card. To edit either one of the cards the command `set` is used followed by the name of the property or information to be edited followed by a value. For example if one would like to generate 100 events the following command is to be executed:

```
set nevents 100
```

Alternatively, both cards can be bypassed by pressing enter and MadGraph5_aMC@NLO continues to run the events and compute a cross section for the process. The running mode of a given process can be returned to an unlimited number of times by launching the process again. The results are Les Houches event (LHE) files containing the unweighted events of the process [21]. In these files data such as the momentum, energy, mass and spin information of the particles included in each event are stored. Moreover, each particle is assigned a unique code called PDGID [22] that allows for identification of the particles present in each event.

2.5 Upper bound on Γ_H using statistical uncertainty

As mentioned in subsection 2.2 the off-shell contribution can be bounded from above by measuring the expected number of events in the off-peak region. Consequently, this allows for derivation of an upper bound on the Higgs width Γ_H by calculating the statistical uncertainty of the expected number of events N_{exp}. The number N of events produced from a process at a hadron collider with a given luminosity L is given by [23]

$$N = \sigma \int dtL, \tag{2.16}$$

where N is equal to the production cross section of the process times the integrated luminosity.

The on-shell cross section $\sigma^{on-shell}$ is dependent on Γ_H and N_{exp} is a function of the cross section. Therefore, the expected number of events in the resonant region is a function of the Higgs width; $N_{exp}(\Gamma_H)$. The computed cross section from MadGraph5_aMC@NLO can be used together with a known integrated luminosity from LHC to calculate N_{exp}. By generating the same signal and altering the width Γ_H for each launch, a range of different $\sigma(\Gamma_H)$ are obtained. As discussed earlier, this changes the on-shell cross section but the off-shell cross section is unchanged when varying Γ_H (see Eq. 2.7). In the on-shell region it is assumed that the cross section is equal to the predicted SM value by Eq. 2.12. To ensure that $\sigma^{on-shell}(\Gamma_H)$ is the same for all Γ_H the total cross section is scaled by a fitting factor λ for each production cross section to align the different cross sections in the on-shell region. This implies that $N_{exp}(\sigma^{on-shell})$ is the same for all Γ_H. What is effectively done is that the coupling constants are scaled by $\mu = \lambda^{1/4}$ to ensure that the on-shell cross sections stay the same for all Γ_H. However, the total cross section has been scaled such that the off-shell cross section increase linearly with $\Gamma_H = \lambda\Gamma_H^{SM}$. Consequently, the expected number of events in the off-shell region is directly proportional to $N_{exp}(\sigma^{off-shell}) \propto \lambda\Gamma_H$ where λ is the scaling factor which the widths are scaled by.

The expected number of events as a function of the invariant mass of the final state leptons in the process $pp \to ZZ \to t\bar{t}4l$ are distributed according to a Poisson distribution. The statistical uncertainty in the off-peak region for the $N_{exp}(\Gamma_H^{SM})$ can be calculated from $\sqrt{N_{exp}(\Gamma_H^{SM})}$. By the linearity $N_{exp} \propto \lambda\Gamma_H$ the Higgs width corresponding to $N_{exp}(\Gamma_H^{SM})$ plus the uncertainty can be extracted at different standard deviations to obtain an upper bound on the Higgs width considering the H signal.

For the derivation of an upper bound considering the total signal, which yields a more realistic result, the contributions from the continuum background, interference and H signal and how their cross sections scale have to be taken into consideration. The total signal and the H signal have to be generated for different Γ_H and the continuum background signal has to be generated. The interference can be calculated from Eq. 2.8 for each Γ_H and scaled according to Eq. 2.9; the interference cross section is proportional to $\sigma_{int} \propto \sqrt{\lambda}$. To keep the on-shell cross section for the process $pp \to ZZ \to t\bar{t}4l$ compatible with the

SM for all widths $\Gamma_H = \lambda\Gamma_H^{SM}$ the total signal cross section has to be reconstructed from its contributions where they are scaled accordingly given by the following equation:

$$\sigma_{tot} = \lambda\sigma_H + \sigma_c + \sqrt{\lambda}\sigma_{int} \tag{2.17}$$

In the same way as explained in the last paragraph, the expected number of events in the off-peak region for each Γ_H can be calculated from the off-peak cross section of the total signal given an integrated luminosity. The statistical uncertainty of $N_{exp}(\Gamma_H)$ in the off-peak region can be calculated and an upper bound on the Higgs width can be found by plotting N_{exp} against Γ_H.

3 Numerical Method

The study of the process $pp \to t\bar{t}4l$ in MadGraph5_aMC@NLO is restricted to computation at LO only. The reason being that the computation time is much lower and not as complicated to perform as NLO computations. Furthermore, LO computations still provide sufficient results for the analysis because the LO terms have the largest contribution to the cross section and dominates over the NLO terms. Moreover, the top quarks are approximated as stable particles by listing them as final state particles when executing the `generate` command. Needless to say the top quark is a highly unstable particle in reality, but it is assumed that it is possible to perfectly reconstruct the top quarks from their decay products, hence simulating them as stable particles. We also simplify the simulations by excluding shower simulations which can be chosen to be turned off in the running mode environment.

3.1 Event generation

The total signal, H signal and continuum background signal were generated respectively by executing the following syntax in the prompt:

```
MG5_aMC> generate p p > t t~ l+ l- l+ l-
MG5_aMC> generate p p > h > t t~ l+ l- l+ l-
MG5_aMC> generate p p > t t~ l+ l- l+ l- / h
```

where `l` denotes an electron or muon, where `l-` is the the negatively charged lepton and `l+` its antiparticle and the `~` sign also indicates an antiparticle. The proton is defined by default to consist of all quarks except bottom and top. The command `display diagrams` was executed in the prompt for the generated H signal. This displays all possible Feynman diagrams for the process.

The cross section for each process was computed with a center of momentum energy for pp collisions at 13 TeV which is the default setting in the run card; each beam has the

energy 6.5 TeV. The number of events to be simulated is set to 10^5 events in order to achieve a statistical significance and at the same time manageable for the program to simulate in a reasonable time. The default cuts on the charged leptons are used, requiring that the transverse momentum $p_T > 10$ GeV and the pseudo-rapidity $|\eta| < 2.5$. In the simulation of these three signals all particles that can be involved are approximated by MadGraph5_aMC@NLO as massless, except the Higgs boson, Z boson and top quark with masses $M_H = 125$ GeV, $M_Z = 91.2$ GeV and $M_t = 173$ GeV specified in the param card. The SM value of decay with of the Higgs boson and the Z boson specified in the param card are numerically estimated by MadGraph5_aMC@NLO to be $\Gamma_H^{SM} = 6.38$ MeV and $\Gamma_Z = 2.44$ MeV at LO. The values differ from the theoretical ones due to NLO effects being neglected. The cross section for each process is computed. The construction of invariant mass histograms from the LHE files of the respective processes is explained in section 3.2.

Thereafter, the generated H signal was launched and the Higgs width was changed each time to values ranging from $\Gamma_H = \Gamma_H^{SM}$ to $\Gamma_H = 8\,\Gamma_H^{SM}$. The multiplicative constant λ was increased in steps of 0.5 for each simulation up to $\lambda = 4$ and then it was increased in steps of 1. This was performed by executing the following command in the prompt:

`>set wh` Γ_H

The same procedure was then performed for the total signal. The LHE files for each simulation were used to obtain the cross sections and conduct the calculations necessary to produce invariant mass histograms (see section 3.2) for the calculation of an upper bound on Γ_H.

3.2 Invariant mass histograms

The LHE file was saved as a txt file. This file contains the computed cross section and data for the 10^5 events generated. A python program was written that reads the file and converts it to a list object containing all the events where each element in the list was constructed as a matrix including the involved particles and their properties. The energy and momentum components of the 4 final state leptons in each event was extracted as a new numpy array with shape (10^5, 4, 4). The invariant mass was calculated by Eq. 2.1. The code is listed in Appendix 7.1.

Histograms of the invariant mass distribution of the three signals were plotted. The histograms were constructed such that each count was assigned a weight equal to the cross section of the specific process divided by the total number of events generated which is 10^5. Similarly, invariant mass histograms for the H signal with different Γ_H were created and on shell cross sections for the different Γ_H were aligned such that they were compatible with the SM. The calculated invariant mass values for each event was divided into two bins: one bin in the on-shell region chosen to be in the range $(120, 130)$ GeV and the other bin in the off-shell region in the range $(130, 2500)$ GeV. The cross sections in both regions were calculated and from the calculated off-shell cross sections $\sigma^{off-shell}$ the expected number

of events N_{exp} were calculated for each process with different Γ_H using an integrated luminosity of 3000 fb^{-1}. The statistical uncertainty of $N_{exp}(\Gamma_H)$ was calculated and the N_{exp} was plotted against Γ_H to obtain an upper bound on the Higgs width.

Thereafter, the analysis of the total signal was conducted to obtain an upper bound on the Higgs width. The same bin size for the on-peak region was used but the bin corresponding to the off-peak region was increased to end at 2800 GeV because there are events in the background signal greater than 2500 GeV. The cross section for the interference given by Eq. 2.8 was calculated for each Γ_H. Thereafter the reconstructed cross section of the total signal for each Γ_H was calculated by Eq. 2.17. The expected number of events N_{exp} were calculated with an integrated luminosity of 3000 fb^{-1} and the statistical uncertainty of $N_{exp}(\Gamma_H)$ was calculated to obtain an upper bound on the Higgs width.

4 Results and Discussion

A representative subset of the Feynman diagrams with a Higgs boson as an intermediate particle are presented in Figure 5. In Figure 6 the SM invariant mass distribution of the 4 final state leptons, which is equal to M_{ZZ}, for the total signal, H signal and continuum background signal is presented. The SM cross sections for the respective signals are listed in Table 2. Only the off peak region is presented in Figure 7 where the behaviour of the cross sections in that region are more clearly displayed.

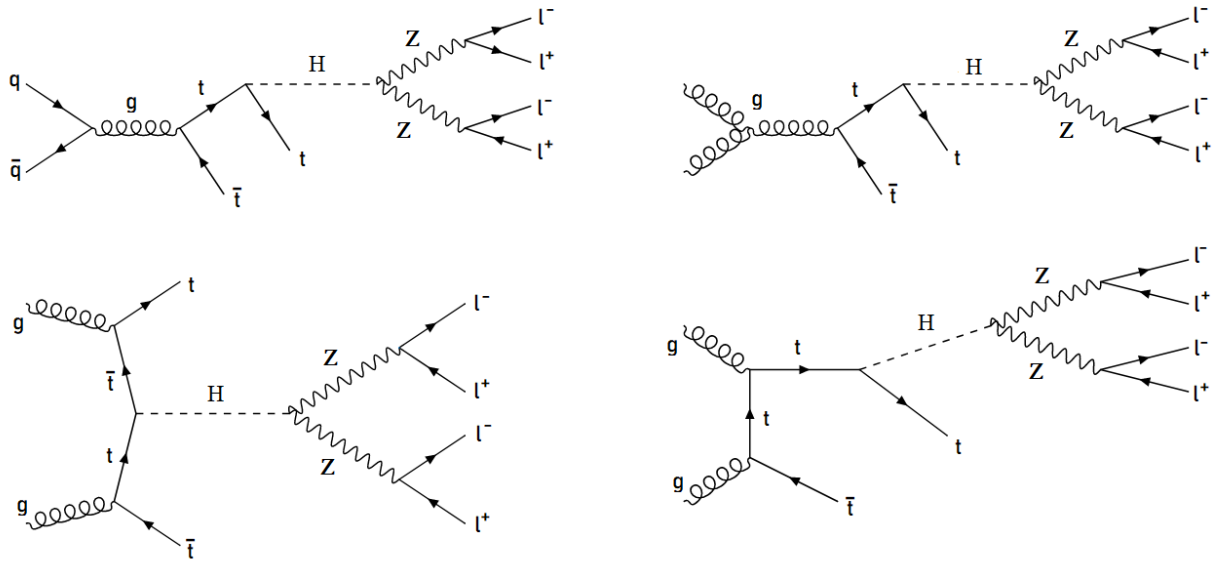

Figure 5: Representative s-channel Feynman diagrams for the H signal generated by executing the command `display diagrams` in MadGraph5_aMC@NLO.

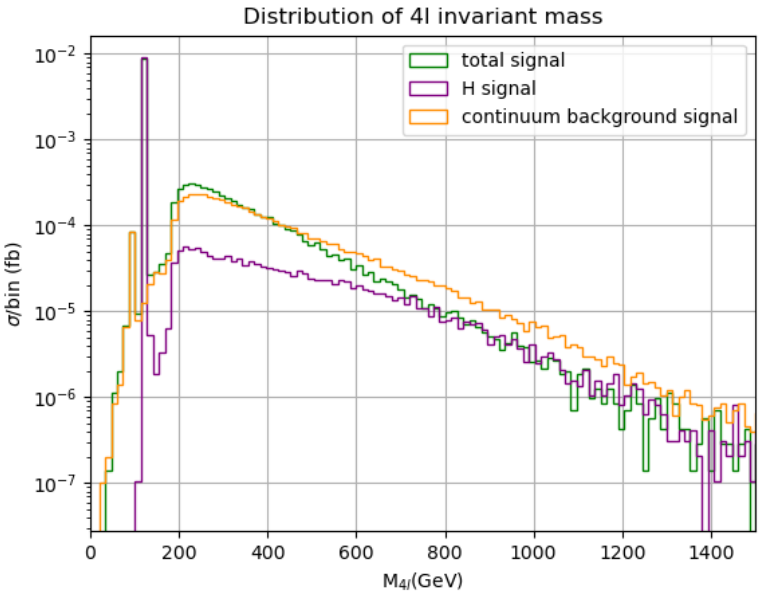

Figure 6: Distribution of the ZZ invariant mass in the $pp \to t\bar{t}4l$ process. Shown in the figure are three log-scaled histograms representing the distribution of the $4l$ invariant mass where $(l = e, \mu)$. These histograms represents the H signal (purple) and the continuum background (orange) contributions to the cross section. The total process (green) represents the sum of both the H signal, continuum background signal and the interference of the two signals.

Signal	σ (fb)
Total	$0.014140 \pm 1.7 \cdot 10^{-5}$
Higgs	$0.010395 \pm 1.8 \cdot 10^{-5}$
Continuum	$0.005045 \pm 4.6 \cdot 10^{-6}$
Interference	$-0.00130 \pm 2.5 \cdot 10^{-5}$

Table 2: This table presents the computed cross sections and the statistical uncertainty of the three generated signals and the cross section of the interference given by Eq. 2.8.

From Figure 6 we note that the cross section in the resonant region for both the total signal and the H signal is practically identical with a difference less than 0.5%. The continuum background contributes significantly to the off-peak cross section and the interference is destructive resulting in a negative cross section for the interference stated in Table 2. Moreover, its importance grows as the invariant mass of ZZ increases.

The on-shell and the off-shell cross sections for the H signal are 0.090 fb and 0.0014 fb respectively, calculated with the cut $M_{4l} < 130$ GeV for the on-peak region and $M_{4l} > 130$ GeV in the off-peak region. This results in a fraction between the cross sections

$\frac{\sigma^{off-shell}}{\sigma^{on-shell}} = 0.16$ compared to a fraction equal to 0.22 for the process $pp \to H \to ZZ \to 4l$ [14]. The reason that the fraction for the process $pp \to t\bar{t}, H \to ZZ \to 4l$ is smaller is probably because a significant amount of energy from the pp collision goes into creating the top quarks such that it reduces the the possibility of Higgs being off shell above its nominal mass. Moreover, the total production cross section is very small which is probably mainly due to the heavy top quarks. That is why a very large integrated Luminosity (3000 fb^{-1}) was used in order to receive a reasonable number of expected events such that an upper bound on Γ_H could be calculated which is presented in subsections 4.1 and 4.2.

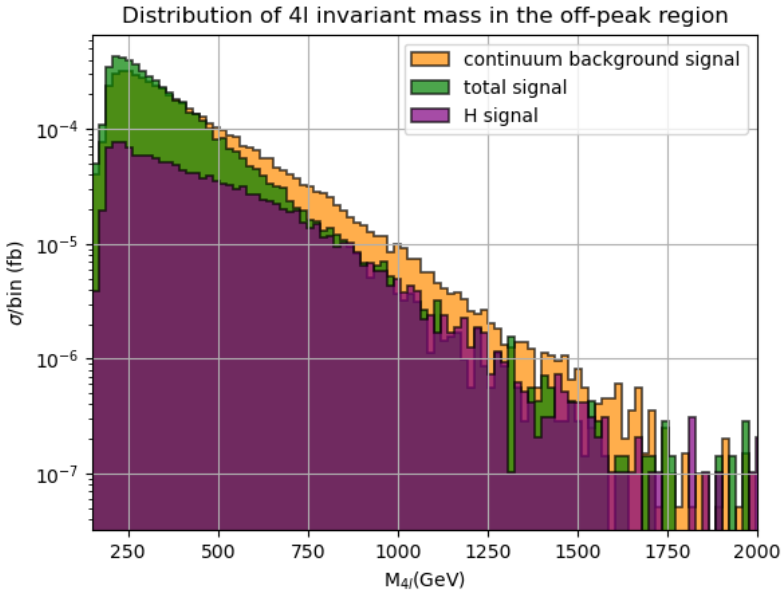

Figure 7: This figure presents the distribution of the ZZ invariant mass in the off peak region up to 2000 GeV. These log-scaled histograms represents the total signal (green), continuum background signal (orange) and the H signal (purple).

From Figure 6 it can be observed that there is a small peak at around 90 GeV from the continuum background contribution. This is probably from an on-shell Z boson decaying to four leptons given by the Feynman diagram in Figure 8.

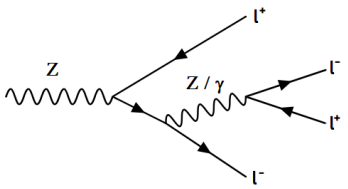

Figure 8: Representative Feynman diagram of an on-shell Z boson representing the peak from the continuum background at an invariant mass of 90 GeV in Figure 6.

In Figure 7 displaying the off-peak region we see how the destructive interference becomes more significant above 500 GeV. Moreover, the cross section for the H signal is quite flat between 200 GeV and 600 GeV while the continuum background has a more decreasing tendency in the entire off-peak region. There are a few events with $M_{4l} > 2500$ GeV which is very large but they are statistically insignificant considering that there are scarcely any events with an invariant mass that large.

4.1 Upper bound on Γ_H considering only the H-signal

In this section the results for the upper bound considering only the H signal are presented. The invariant mass distributions for the H signal for four different Higgs widths are presented in Figure 9. These figures clearly display how the off-shell cross section is not dependent on the Higgs width and then by assuming that the on-shell cross section is compatible with SM for all Γ_H the off-shell cross section increases with the scaling. This results in an increasing expected number of events in that region as the width increases. In Table 3 the statistical uncertainty of the cross section given by MadGraph5_aMC@NLO is not included because it is very small on the order of $(10^{-5} - 10^{-6})$ fb as can be seen in Table 2. Instead, less significant digits are used such that the error does not affect the result. The same is true for Table 4 in the next subsection where the total signal is considered.

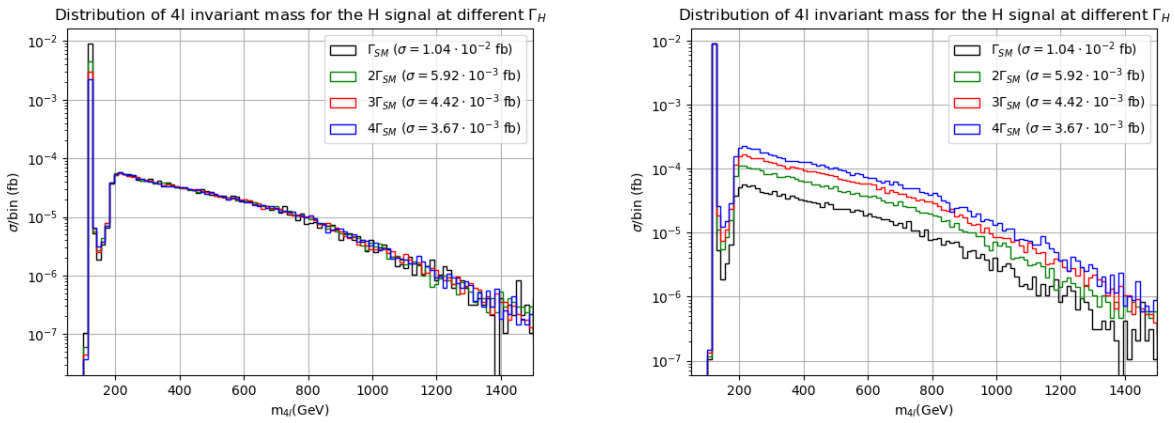

Figure 9: The invariant mass distribution of the H signal with different Higgs widths. In the left hand figure four log-scaled histograms are presented where the Higgs width ranges from $\Gamma_H = \Gamma_H^{SM}$ to $\Gamma_H = 4\Gamma_H^{SM}$. In the right hand figure the cross sections are normalized such that the on-shell cross sections are equal for all processes.

The cross section in the on-shell region was observed to be $\sigma^{on-shell} = 0.00897$ fb. In Table 3 the calculated off shell cross sections $\sigma^{off-shell}$ and the corresponding number of expected events for the H signal are presented.

Γ_H	$\sigma_H^{off-shell}$ (fb)	N_{exp}
Γ_H^{SM}	0.00143	4.29
$1.5\Gamma_H^{SM}$	0.00213	6.39
$2.0\Gamma_H^{SM}$	0.00284	8.52
$2.5\Gamma_H^{SM}$	0.00353	10.6
$3.0\Gamma_H^{SM}$	0.00426	12.8
$3.5\Gamma_H^{SM}$	0.00500	15.0
$4.0\Gamma_H^{SM}$	0.00570	17.1

Table 3: This table presents the calculated off-shell cross sections and the expected number of events for different Higgs widths with an integrated luminosity of 3000 fb^{-1}. The on-shell cut is 120 GeV $\geq M_{4l} \leq$ 130 GeV and the off-shell cut is $M_{4l} \geq$ 130 GeV.

The statistical uncertainty of the expected number of events for the SM width is $\sqrt{N_{exp}(\Gamma_H^{SM})} = 2.069$. The linear fit of the expected number of events against the Higgs width is shown in Figure 10.

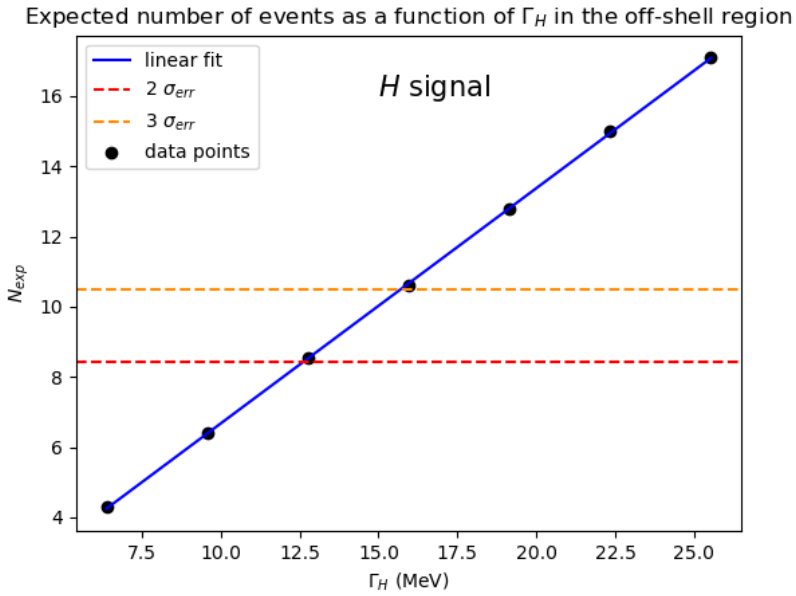

Figure 10: In this figure a linear regression of the expected number of events from the H signal versus the Higgs width Γ_H is presented. The black dots represent the calculated number of events for different Γ_H presented in Table 3 and the blue line is a linear fit to those values. The red and yellow horizontal dotted lines represent the expected number of events two standard deviations $2\sigma_{err}$ and three standard deviations $3\sigma_{err}$ respectively above the expected number of events for the SM width $\Gamma_H = \Gamma_H^{SM}$.

Requiring that the expected number of events are within 2 standard deviations and 3

standard deviations from $N_{exp}(\Gamma_H^{SM})$, we find an upper bound on the Higgs width at the 95% and 99.7% confidence level respectively:

$$\Gamma_H \leq 1.98\,\Gamma_H^{SM}, \quad \Gamma_H \leq 2.46\,\Gamma_H^{SM}. \tag{4.18}$$

4.2 Complete analysis of the upper bound on Γ_H

This subsection provides the results for the derivation of an upper bound on the Higgs width considering the total signal. Hence, these results are more physical than the results for the upper bound considering the H signal alone because at LHC the H signal and continuum background can not be distinguished from the total signal. What would be measured at the detectors at the LHC is the final state leptons and decay products from the top quarks (we assume the top quarks to be stable) corresponding to the process $pp \to t\bar{t}4l$ which is the total signal.

In Table 4 the off-peak cross sections for the reconstructed total signal for different Higgs widths are presented together with the expected number of events. The linear fit to the calculated expected number of events as a function of Γ_H is presented in Figure 11.

Γ_H	$\sigma_{tot}^{off-peak}$ (fb)	N_{exp}
Γ_H^{SM}	0.00511	15.3
$1.5\Gamma_H^{SM}$	0.00551	16.5
$2.0\Gamma_H^{SM}$	0.00597	17.9
$2.5\Gamma_H^{SM}$	0.00644	19.3
$3.0\Gamma_H^{SM}$	0.00703	21.1
$3.5\Gamma_H^{SM}$	0.00760	22.8
$4.0\Gamma_H^{SM}$	0.00811	24.3
$5.0\Gamma_H^{SM}$	0.00927	27.8
$6.0\Gamma_H^{SM}$	0.01044	31.3
$7.0\Gamma_H^{SM}$	0.01165	34.9
$8.0\Gamma_H^{SM}$	0.01286	38.6

Table 4: This table presents the calculated off-shell cross sections and expected number of events for the total signal for different Higgs widths with an integrated luminosity of 3000 fb^{-1}. The same invariant mass cuts as in Table 3 are used.

The statistical uncertainty for the expected number of events corresponding to the SM width is 3.91. The expected number of events in the off-peak region for the total signal presented in Table 4 are larger than N_{exp} for the H signal only, presented in Table 3, because the contribution from the continuum background greatly enhances the expected number of events which results in a larger statistical uncertainty. Moreover, the on-peak cross section for the total signal is 0.00892 fb for the SM width. Then with increasing width as the contributions to the on-peak cross section are scaled according to Eq. 2.17

the 5th decimal place varies a bit because the interference still exists in the peak but can be approximated as statistically irrelevant as it is tiny in that region. That is the same reasoning used to justify not including the statistical uncertainty of the computed cross sections.

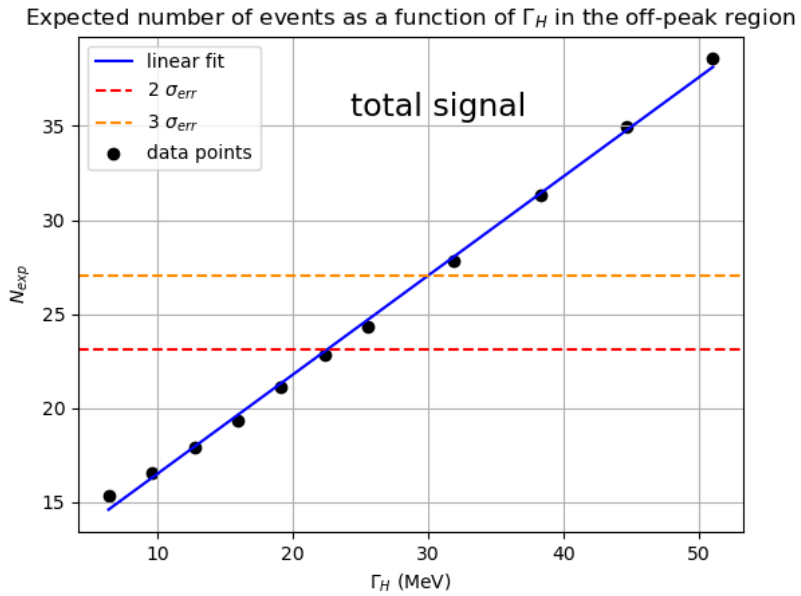

Figure 11: The expected number of events N_{exp} from the total signal are plotted against the Higgs width. The black dots represent the calculated expected number of events for different Γ_H presented in Table 4 and the blue line is a linear fit to those values. The red and yellow horizontal dotted lines represent the expected number of events two standard deviations $2\sigma_{err}$ and three standard deviations $3\sigma_{err}$ respectively above the expected number of events for the SM width $\Gamma_H = \Gamma_H^{SM}$.

From Figure 11 we obtain an upper bound on the Higgs width for the process $pp \to t\bar{t}4l$ at the 95% and 99.7% confidence level respectively:

$$\Gamma_H \leq 3.54\,\Gamma_H^{SM}, \quad \Gamma_H \leq 4.70\,\Gamma_H^{SM}. \tag{4.19}$$

The upper bound on Γ_H results in an upper limit on the branching ratio to invisible final states given by Eq. 2.14 and it is $BR_{inv} \leq 0.47$ at the 95% confidence level. Note that the upper bound on Γ_H was derived by using the total number of events observed in $pp \to t\bar{t}4l$ in a very broad range of four-lepton invariant masses from 130 GeV to 2800 GeV. It may be the case that this is not an optimal range to choose considering the behaviour of the off-peak cross section (see Figure 7). With more careful selection of the invariant mass range used for this type of analysis we believe that the upper bound presented in Eq. 4.19 might be improved. Moreover, the on-peak region could possibly be defined

more rigorously to attain more accurate results. We define it as all events with a four-lepton invariant mass between 120 GeV and 130 GeV which symmetrically contains the on-shell mass of the Higgs boson. However the resonant region for the Higgs boson is much smaller since the width is in orders of MeV. As pointed out before the cross section for the process is very small (see Table 2). Setting the beam energy to a larger value would of course increase the cross section. We used a total collision energy of 13 TeV and what is achievable at the LHC today is up to 13.6 TeV. If generating the events with a collision energy of 14 TeV for example, the cross section for the process would be 19% larger which would only result in approximately 3 more events in the off-peak region. Another thing that would change the cross section is the selection cuts of the transverse momentum of the final state leptons and the pseudo-rapidity. If the cut of the transverse momentum would be decreased, allowing for final state leptons with lower transverse momentum, the total cross section would increase but the fraction of off-shell Higgs events would be lower. From MadGraph5_aMC@NLO we find that when using the cut $p_T > 7$ GeV instead of $p_T > 10$ GeV the SM cross section becomes almost 40% larger but the fraction of off-shell events are only 0.11 compared to 0.16 for the cut $p_T > 10$ GeV.

Nevertheless, the calculated upper bound on the Higgs width is quite small compared to similar studies for other processes. To this end we have to keep in mind that the integrated luminosity is chosen as an arbitrary value in order to obtain a significant number of expected events such that the analysis could be conducted. It is expected that the LHC could reach an integrated luminosity around 3000 fb^{-1} in approximately 20 years. With large luminosity one can expect the error in the number of expected events to be dominated by systematic uncertainties. Moreover, polarization effects are not taken into account and they could play a substantial role at high invariant masses. The reason is that when the Z bosons are produced from off-shell Higgs bosons they are most likely longitudinally polarized [14].

Systematic uncertainties are not taken into account at all in this thesis, only the statistical uncertainty allowing for an upper boundary. There are a lot of systematic uncertainties due to several assumptions and approximations made when generating the events in MadGraph5_aMC@NLO. There are three major approximations made. Firstly, that we have assumed an ideal detector; we can perfectly measure the desired process because there is no background noise. In real detectors all possible interactions from a pp collision are observed and a challenge is to try to filter out all the background noise and single out the process in interest. Secondly, as mentioned before, we assume that the top quarks can be perfectly reconstructed from their decay products and hence we treat them as stable particles. We force the top quarks to be detected as stable particles when we generate the events in MadGraph5_aMC@NLO. Lastly, we make the approximation to restrict ourselves to LO computations as discussed in section 3. If the NLO and NNLO QCD would be considered the result would of course be more accurate. To comment on the first assumption, a benefit with having the top quarks in the finals state is that it reduces the background noise in a real detector because a larger fraction of the measured particles would correspond to the desired process.

There are also uncertainties coming from how MadGraph5_aMC@NLO computes cross sections and the fact that we do not include all possible particles in $pp \to t\bar{t}4l$. The first uncertainty being that an equal probability is assigned for all possible events to occur. That is not necessarily true in reality. We also do not consider the Tau leptons in the final state leptons and the protons are defined to not consist of bottom quarks. If the Tau leptons were included and measured they would contribute to a larger total cross section because there would be more possible decay channels. It would result in more expected events, thus, leading to a larger statistical uncertainty such that a more accurate result of the upper bound could be obtained. Nevertheless, the calculated cross section in MadGraph5_aMC@NLO when including the Tau leptons is 0.036 fb^{-1} which still is very small compared to other Higgs processes without the top quarks. However, the cross section increased with more than 100% when including the Tau leptons. In addition, the Tau leptons are much more difficult to measure in a real detector because they can decay to hadrons, thus it becomes difficult to reconstruct them. Moreover, including the bottom quarks might change the cross section but only a tiny amount.

5 Conclusion

In this thesis we have calculated an upper bound on the Higgs width considering Higgs production associated with a top quark pair. The total signal and its contributions from the Higgs signal and the continuum background signal have been generated in MadGraph5_aMC@NLO and their cross sections have been computed. The destructive contribution to the cross section from the interference have been calculated as well. All the contributions have been studied in a broad range of the four-lepton invariant masses and the off-peak cross section has been calculated for different Higgs widths. The contribution from the H signal alone was studied first. By assuming that all on-shell cross sections for different widths are compatible with the SM, which they can be when making a cross section measurement, the total number of expected events in the off-shell region could be calculated which resulted in an upper bound on the Higgs width with the 95% confidence level: $\Gamma_H \leq 1.98\,\Gamma_H^{SM}$. The more realistic analysis of the total signal, corresponding to the process in interest, considering all the contributions were then conducted. By reconstructing the total signal cross section by scaling the contributions accordingly for the different Γ_H an upper bound on the Higgs width at the 95% confidence level was found to be $\Gamma_H \leq 3.54\,\Gamma_H^{SM}$. This result translates into a branching ratio to invisible final states $BR_{inv} \leq 0.47$. These results were found by considering the statistical uncertainty of the expected number of events of the process with the SM Higgs width. The upper bound derived is small which is good and we believe our results are sufficiently accurate. However, there are several approximations made which decrease the accuracy of the results. Our study ignores many details of event selection and predominantly we assume the detector to be ideal and that the top quarks are stable particles measured at the detector.

Not until approximately 2040 when an integrated luminosity of about 3000 fb^{-1} is achiev-

able would it be possible to have enough events for this process at LHC due to the tiny cross section. However, when that is possible, there are other Higgs processes not including top quarks which would generate significantly more events and thus they would be better in order to measure the Higgs width. Despite that, a benefit with having the top quarks is that they reduce the background noise. In this thesis we have set a constraint on the Higgs width accurately enough such that scientists at LHC, when it is time to generate $pp \to t\bar{t}4l$ would know that the Higgs width can not be larger than 3.5 times the SM value with up to a 95% confidence level.

6 Acknowledgements

I am grateful for Fabrizio Caola and Kirill Melnikov for pointing out and explaining that a model independent upper bound on the Higgs width can be derived thanks to strongly enhanced off-shell contributions. To my supervisor Rikkert Frederix who provided great discussions and good insights into difficult topics and made them easy to understand. He granted me with helpful feedback to advance and elevate my bachelor project but he also left many things open for me to think about and evidently choose the path I wanted to go. It was a good mixture of a lot of independent work from my side and supportive inputs from Rikkert when it was needed. Thank you for that. I also want to thank Matilda Fors, Melvin Tham, Oskar Nilsson, Filip Gustavsson, Eric Svensson, Johan Holmberg, Elliot Winsnes, Claudia Skoglund and Matilda Skantz for their support through tough and stressful times.

References

[1] Steven Weinberg. "A Model of Leptons". In: *Phys. Rev. Lett.* 19 (21 Nov. 1967), pp. 1264–1266. DOI: 10.1103/PhysRevLett.19.1264.

[2] F. Englert and R. Brout. "Broken Symmetry and the Mass of Gauge Vector Mesons". In: *Phys. Rev. Lett.* 13 (9 Aug. 1964), pp. 321–323. DOI: 10.1103/PhysRevLett.13.321.

[3] Peter W. Higgs. "Broken Symmetries and the Masses of Gauge Bosons". In: *Phys. Rev. Lett.* 13 (16 Oct. 1964), pp. 508–509. DOI: 10.1103/PhysRevLett.13.508.

[4] G. S. Guralnik, C. R. Hagen, and T. W. B. Kibble. "Global Conservation Laws and Massless Particles". In: *Phys. Rev. Lett.* 13 (20 Nov. 1964), pp. 585–587. DOI: 10.1103/PhysRevLett.13.585.

[5] ATLAS Collaboration. "Observation of a new boson at a mass of 125 GeV with the CMS experiment at the LHC". In: *Physics Letters B* 716.1 (Sept. 2012), pp. 30–61. DOI: 10.1016/j.physletb.2012.08.021.

[6] CMS Collaboration. "Observation of a new boson at a mass of 125 GeV with the CMS experiment at the LHC". In: *Physics Letters B* 716.1 (Sept. 2012), pp. 30–61. DOI: 10.1016/j.physletb.2012.08.021.

[7] Gordon Kane. *Modern Elementary Particle Physics*. 2nd ed. Cambridge: Cambridge University Press, 2017. Chap. 15.1.

[8] Tommaso Dorigo. "Recent CMS Results". In: *EPJ Web Conf.* 71 (2014). Ed. by L. Bravina, Y. Foka, and S. Kabana, p. 00041. DOI: 10.1051/epjconf/20147100041.

[9] CERN. *CERN Yellow Reports: Monographs, Vol 2 (2017): Handbook of LHC Higgs cross sections: 4. Deciphering the nature of the Higgs sector*. en. 2017. DOI: 10.23731/CYRM-2017-002.

[10] Armen Tumasyan et al. "Measurement of the Higgs boson width and evidence of its off-shell contributions to ZZ production". In: *Nature Phys.* 18.11 (2022), pp. 1329–1334. DOI: 10.1038/s41567-022-01682-0.

[11] J. Alwall et al. "The automated computation of tree-level and next-to-leading order differential cross sections, and their matching to parton shower simulations". In: *JHEP* 07 (2014), p. 079. DOI: 10.1007/JHEP07(2014)079.

[12] Gordon Kane. *Modern Elementary Particle Physics*. 2nd ed. Cambridge: Cambridge University Press, 2017. Chap. 9.2.

[13] Gordon Kane. *Modern Elementary Particle Physics*. 2nd ed. Cambridge: Cambridge University Press, 2017. Chap. 10.1.

[14] Fabrizio Caola and Kirill Melnikov. "Constraining the Higgs boson width with ZZ production at the LHC". In: *Phys. Rev. D* 88 (2013). DOI: 10.1103/PhysRevD.88.054024.

[15] Duane A. Dicus and Scott S. D. Willenbrock. "Photon pair production and the intermediate-mass Higgs boson". In: *Phys. Rev. D* 37 (7 Apr. 1988), pp. 1801–1809. DOI: 10.1103/PhysRevD.37.1801.

[16] John M. Campbell, R. Keith Ellis, and Ciaran Williams. "Gluon-gluon contributions to W W - production and Higgs interference effects". In: *Journal of High Energy Physics* 2011.10 (Oct. 2011). DOI: 10.1007/jhep10(2011)005.

[17] Nikolas Kauer and Giampiero Passarino. "Inadequacy of zero-width approximation for a light Higgs boson signal". In: *Journal of High Energy Physics* 2012.8 (Aug. 2012). DOI: 10.1007/jhep08(2012)116.

[18] "Precision electroweak measurements on the Z resonance". In: *Physics Reports* 427.5-6 (May 2006), pp. 257–454. DOI: 10.1016/j.physrep.2005.12.006.

[19] ATLAS Collaboration. "Measurement of the top-quark mass in t\overline{t} 1-jet events collected with the ATLAS detector in pp collisions at \sqrt{s} = 8 TeV". In: *Journal of High Energy Physics* 2019.11 (Nov. 2019). DOI: 10.1007/jhep11(2019)150.

[20] Neil D. Christensen and Claude Duhr. "FeynRules – Feynman rules made easy". In: *Computer Physics Communications* 180.9 (Sept. 2009), pp. 1614–1641. DOI: 10.1016/j.cpc.2009.02.018.

[21] J. Alwall et al. "A standard format for Les Houches Event Files". In: *Computer Physics Communications* 176.4 (Feb. 2007), pp. 300–304. DOI: 10.1016/j.cpc.2006.11.010.

[22] L. Garren et al. "Monte Carlo particle numbering scheme: in Review of Particle Physics (RPP 2000)". In: *Eur. Phys. J. C* 15 (2000), pp. 205–207. DOI: 10.1007/BF02683426.

[23] Gordon Kane. *Modern Elementary Particle Physics*. 2nd ed. Cambridge: Cambridge University Press, 2017. Chap. 12.1.

7 Appendix

7.1 Invariant mass histograms

```
import numpy as np
import matplotlib.pyplot as plt

# total signal
def event():
    with open("unweighted_events SM total.txt","r") as f:
        file=f.readlines()

    # locates rows before and after the information about the events
    start=[i for i in range(len(file)) if "<event>" in file[i]]
    stop=[i for i in range(len(file)) if "<mgrwt>" in file[i]]

    #creates an useable list object with only the important information in the file; all events
    data=["".join(file[start[j]+2:stop[j]]) for j in range(len(start))]

    new_data = [data[j].split() for j in range(len(data))]

    new_data=[np.array(list(map(float,new_data[j]))).reshape((-1,13))
              for j in range(len(new_data))]

    return new_data

data=event() # list of all events where each entry in the list is a numpy array

N=len(data)

#calculate invariant mass
def inv_mass():
    final_states=[data[j][-4:] for j in range(N)]  #extracts 4 final state leptons
    four_momenta=np.array([final_states[j][:,6:10] for j in range(N)]) #momenta of the 4 leptons

    sum_p=np.sum(four_momenta[:,:,0:3],axis=1) #sum of the momenta of the leptons

    norm_p=(np.linalg.norm(sum_p[:,:],axis=-1)**2).reshape((N,1)) #norm of summed momentum

    E=(np.sum(four_momenta[:,:,3],axis=1)**2).reshape(N,1) #sum of the energy of the leptons

    W=np.sqrt(E-norm_p) #the invariant mass of the final state leptons

    return W

W=inv_mass() #invariant mass distribution for total signal


#£H£ signal
def event_higgs():
```

```
    with open("unweighted_events $H$ signal SM.txt","r") as f:
        file=f.readlines()

    start=[i for i in range(len(file)) if "<event>" in file[i]]
    stop=[i for i in range(len(file)) if "<mgrwt>" in file[i]]

    data=["".join(file[start[j]+2:stop[j]]) for j in range(len(start))]

    new_data = [data[j].split() for j in range(len(data))]

    new_data=[np.array(list(map(float,new_data[j]))).reshape((-1,13))
              for j in range(len(new_data))]

    return new_data

datahiggs=event_higgs()

def inv_mass1():
    final_states=[datahiggs[j][-4:] for j in range(N)]
    four_momenta=np.array([final_states[j][:,6:10] for j in range(N)])

    sum_p=np.sum(four_momenta[:,:,0:3],axis=1)

    norm_p=(np.linalg.norm(sum_p[:,:],axis=-1)**2).reshape((N,1))

    E=(np.sum(four_momenta[:,:,3],axis=1)**2).reshape(N,1)

    W=np.sqrt(E-norm_p)

    return W

W1=inv_mass1() #invariant mass distribution for £H£ signal


#Continuum background signal
def event_nohiggs():
    with open("unweighted_events background.txt","r") as f:
        file=f.readlines()
    start=[i for i in range(len(file)) if "<event>" in file[i]]
    stop=[i for i in range(len(file)) if "<mgrwt>" in file[i]]

    data=["".join(file[start[j]+2:stop[j]]) for j in range(len(start))]

    new_data = [data[j].split() for j in range(len(data))]

    new_data=[np.array(list(map(float,new_data[j]))).reshape((-1,13))
              for j in range(len(new_data))]

    return new_data

datanohiggs=event_nohiggs()
```

```
def inv_mass2():
    final_states=[datanohiggs[j][-4:] for j in range(N)]
    four_momenta=np.array([final_states[j][:,6:10] for j in range(N)])

    sum_p=np.sum(four_momenta[:,:,0:3],axis=1)

    norm_p=(np.linalg.norm(sum_p[:,:],axis=-1)**2).reshape((N,1))

    E=(np.sum(four_momenta[:,:,3],axis=1)**2).reshape(N,1)

    W=np.sqrt(E-norm_p)

    return W

W2=inv_mass2() #invariant mass distribution for continuum background signal


#plots histograms where each signal is weighted according to its cross section
def hist_tot():
    num_bins=np.linspace(0,2800,200)

    #total signal
    n,bins,patches=plt.hist(W,num_bins, weights= (1.4140252578174647e-02/N)*np.ones((N,1)),
                   log=True, histtype='step',label='total signal',color='green')

    #£H£ signal
    n1,bins1,patches=plt.hist(W1,num_bins, weights=(1.03949462e-02/N)*np.ones((N,1)),
                     log=True, histtype='step',label='$H$ signal',color='purple')

    #continuum background signal
    n2,bins2,patches=plt.hist(W2,num_bins, weights=(5.04459659225112e-03/N)*np.ones((N,1)),
            log=True, histtype='step',label='continuum background signal',color='darkorange')

    interference=n-n1-n2 #calculates interference cross section

    print(sum(n))  #prints cross section for total signal
    print(sum(n1)) #prints cross section for £H£ signal
    print(sum(n2)) #prints cross section for continuum background signal
    print(sum(interference)) #prints cross section for interference

    plt.ylabel('$\sigma $/bin (fb)')
    plt.xlabel('M$_{4l}$(GeV)')
    plt.xlim(0,2500)
    plt.title('Distribution of 4l invariant mass')
    plt.grid()
    plt.legend()

hist_tot()
```